Pb electrodeposition on polycrystalline Cu in the presence and absence of Cl⁻: A combined oblique incidence reflectivity difference and in situ AFM study

Guang Yu Wu [a], S.-E. Bae [b], A.A. Gewirth [b], J. Gray [c], X.D. Zhu [c],
T.P. Moffat [d], W. Schwarzacher [a,*]

[a] *H.H. Wills Physics Laboratory, University of Bristol, Bristol BS8 1TL, UK*
[b] *Department of Chemistry and Frederick Seitz Materials Research Laboratory, University of Illinois at Urbana-Champaign, Urbana, IL 61801, USA*
[c] *Department of Physics, University of California, Davis, CA 95616, USA*
[d] *National Institute of Standards and Technology, Materials Science and Engineering Laboratory, Gaithersburg, MD 20899, USA*

Abstract

Oblique incidence reflectivity difference (OI-RD) measurements reveal differences in the earliest stages of overpotential-deposited (OPD) growth between Pb electrodeposition on polycrystalline Cu surfaces in the presence and absence of Cl⁻. At moderate overpotentials, when only 100 mM ClO_4^- is present, the magnitude of the real part of the OI-RD signal continues to increase after completion of the first underpotential-deposited (UPD) Pb monolayer, but with the addition of 20 mM KCl the magnitude decreases after the UPD monolayer forms. In situ atomic force microscopy (AFM) shows that in the former case the island density is much greater than in the latter. Using OI-RD as a probe, we show additionally that when the substrate potential is returned to a more positive potential in the presence of Cl⁻, the UPD Pb monolayer dissolves after the Pb islands disappear.
© 2007 Elsevier B.V. All rights reserved.

Keywords: Atomic force microscopy; Electrochemical methods; Ellipsometry; Electrochemical phenomena; Nucleation; Lead; Copper

1. Introduction

Under ultrahigh vacuum (UHV) conditions, previous studies have shown that Pb grows layer-by-layer on Cu(1 1 1) at low temperatures (e.g., 140 K), stabilized by the quantum size effect [1,2]. LEED studies showed that the lattice parameter of the first Pb monolayer is slightly less than that of bulk Pb. At $T \geqslant 300$ K, the energy penalty associated with pseudomorphic growth on this compressed substrate favours the subsequent growth of relaxed 3-D Pb islands (Stranski–Krastanov growth) [2]. When Pb is electrodeposited on Cu(1 1 1) or Cu(1 0 0), the growth of the ini-

tial monolayer at a deposition potential positive of the bulk deposition potential is also distinct from subsequent growth. The structure and properties of this underpotential-deposited (UPD) monolayer have been studied extensively. Brisard et al. have shown that Pb UPD on Cu in a chloride-containing electrolyte is accompanied by Cl⁻ desorption [3,4]. Chu et al. used in situ surface X-ray diffraction (XRD) to demonstrate that the UPD Pb monolayer on Cu(1 1 1) is also compressed compared to bulk Pb, as for the first monolayer in vacuum deposition [5]. Moffat has shown that the early stages of Pb UPD on Cu(0 0 1) were accompanied by surface alloy formation [6], and the same might be expected for Pb UPD on Cu(1 1 1) as UHV experiments have already demonstrated surface alloy formation for Pb deposition on both the (1 1 1) and (0 0 1) faces of Cu [7,8].

In contrast to Pb UPD on Cu, very little attention has been paid to the subsequent growth of Pb at potentials negative of the bulk deposition potential, *i.e.*, overpotential deposition (OPD). Here we present the results of such a study for Pb OPD on polycrystalline Cu in the presence and absence of chloride, using a combination of oblique incidence reflectivity difference (OI-RD) and in situ AFM. OI-RD is a form of polarization-modulation ellipsometry (PME), optimized to probe changes that take place at the surface of a substrate [9,10]. The essential difference between OI-RD and conventional PME is that, prior to an experiment, the Pockels cell and polarizer are used to nullify the first and second harmonics of the phase-modulated light. Its sub-monolayer sensitivity and speed means that it can be used to follow the early stages of electrodeposition processes even involving fast kinetics. OI-RD has been used to study the electrodeposition of Co on Au [11] and to characterize gas adsorption and film growth under UHV conditions [9,10,12]. However, like most optical measurements, the interpretation of OI-RD results relies on appropriate knowledge of the surface morphology of the thin-film system under investigation [13,14]. We have, therefore, used in situ AFM to interpret the data from the OI-RD measurements.

We find that for the Pb on Cu system studied, the OI-RD signal is dependent on the deposition potential, and whether Cl^- is present in the electrolyte. With the help of in situ AFM, we show that the observed differences in the OI-RD signal are due to dramatic differences in the density and the average size of 3-D islands formed during OPD. The combination of AFM and OI-RD makes an extremely powerful tool for electrodeposition studies.

2. Experimental

The experimental arrangement for OI-RD is shown in Fig. 1. Light from a 15 mW He–Ne laser passes through a polarizer and is then modulated by the photoelastic modulator (PEM90, Hinds Instruments) between p- (electric field parallel to the reflection plane) and s- (electric field perpendicular to the reflection plane) at a frequency of $\Omega = 50$ kHz
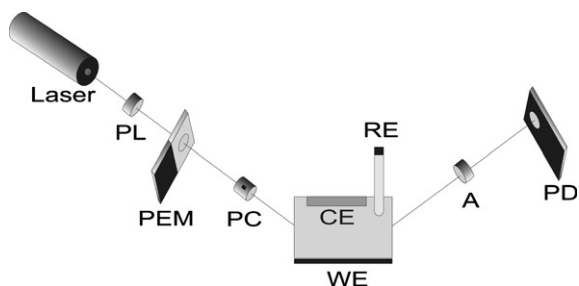

Fig. 1. Sketch of the electrochemical cell and optical set up for the oblique incidence reflectivity difference experiment. Laser: 15 mW He–Ne laser; PL: Glan-Thompson polarizers; PEM: photoelastic modulator (Hinds Instruments); PC: Pockels cell; CE: counter electrode; RE: reference electrode; WE: working electrode (Cu/Au/glass); A: analyzer; PD: biased silicon photodiode.

before passing through a Pockels cell. After reflection from the sample, the light passes through an analyzer before being detected by the photodiode. The measured intensity has terms in various harmonics of the modulation frequency Ω, and during an OI-RD experiment we monitor $I(2\Omega)$ using a lock-in amplifier. We used a computer-aided data acquisition system to collect the optical and electrochemical data simultaneously. Prior to electro-deposition, the transmission axis of the analyser and the Pockels cell are adjusted so that $I(2\Omega)$ is close to zero. $I(2\Omega)$ is proportional to the real part of $\Delta_p - \Delta_s$, i.e., $\text{Re}\{\Delta_p - \Delta_s\}$, where we define $\Delta_p = (r_p - r_{p0})/r_{p0}$ and $\Delta_s = (r_s - r_{s0})/r_{s0}$, with r_p and r_s being the sample reflectivity for p- and s-polarized light during electrodeposition and r_{p0} and r_{s0} the corresponding values for the substrate [10]. For a simple three-layer system (substrate–film–electrolyte), $\text{Re}\{\Delta_p - \Delta_s\}$ is proportional to the film thickness for an optically smooth film, and depends on the optical dielectric constants of the substrate, the film, and the electrolyte [9].

For in situ AFM measurements, a Molecular Imaging PicoSPM 300 was used working in contact mode with cantilevers having a force constant of 0.58 N m^{-1}. Images were acquired over areas of either $15\,\mu m \times 15\,\mu m$ or $30\,\mu m \times 30\,\mu m$ with a resolution of 256×256 pixels.

Cu/Au/glass substrates were prepared by vacuum evaporation of an Au film onto a glass microscope slide. A 100 nm thick Cu film was then deposited on the Au from a 0.3 M $CuSO_4$/1.2 M H_2SO_4 electrolyte containing trace Cl^- at a current density of 20 mA cm^{-2}. The Cu substrate was washed with pure water and dried with N_2 before being immersed into the Pb electrolyte and held at a potential of -0.2 V prior to Pb deposition. For the Pb electrodeposition experiments we prepared perchlorate-based electrolytes containing 100 mM $HClO_4$ (perchloric acid) + 1 mM Pb^{2+} (from either lead perchlorate $Pb(ClO_4)_2$ or lead oxide PbO). Electrolytes were prepared using ultrapure water and 99.999% $HClO_4$ to minimize chloride contamination. For some experiments, we deliberately added chloride in the form of 20 mM KCl. Electrodeposition experiments were carried out either in the optical cell shown in Fig. 1, or in the AFM cell. In the optical cell we used a saturated calomel (SCE) or mercury sulphate (MSE) reference electrode while in the AFM cell we used a Pb wire as a reference.[1] All potentials are quoted with respect to SCE.

3. Results and discussion

Fig. 2a and b show cyclic voltammograms (CV) obtained at a rate of 10 mV/s, in a solution containing 100 mM $HClO_4$ and 1 mM $Pb(ClO_4)_2$ with and without 20 mM KCl, respectively. Although there are differences in the precise peak positions, qualitatively, our results are in good agreement with earlier studies on Cu single crystals

---

[1] Although the SCE could introduce trace chloride to our nominally chloride-free electrolyte, it did not make any noticeable difference to our results whether this or the MSE was used.
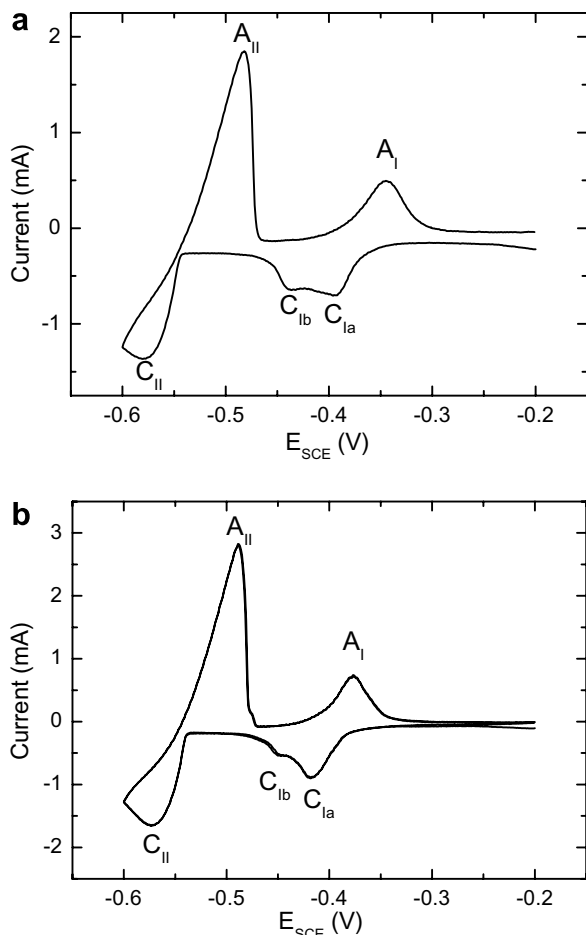
Fig. 2. Cyclic voltammograms for a (1 1 1)-textured polycrystalline Cu substrate measured in: (a) 100 mM $HClO_4$ + 1 mM $Pb(ClO_4)_2$; (b) 100 mM $HClO_4$ + 1 mM $Pb(ClO_4)_2$ + 20 mM KCl. The scan rate was 10 mV s^{-1} and all potentials are quoted with respect to SCE.

Fig. 3. OI-RD signal $|Re\{\Delta_p - \Delta_s\}|$ (not normalized) recorded when stepping the Cu substrate potential (a) from $E = -0.2$ V to $E = -0.5$ V for $t = 50$ s (underpotential deposition – UPD) and (b) from $E = -0.2$ V to $E = -0.54$ V for $t = 50$ s (overpotential deposition – OPD). The electrolyte was 100 mM $HClO_4$ + 1 mM $Pb(ClO_4)_2$.

[3,4]. In both CV's a double-peak structure labelled 'C_{Ia}' and 'C_{Ib}' is seen during the cathodic scan around -0.4 V, corresponding to Pb UPD, while bulk deposition commences at ~-0.54 V. Peaks corresponding to bulk and UPD Pb dissolution, labelled 'A_{II}' and 'A_I' respectively are seen during the anodic scan. In agreement with studies on single crystal substrates, the splitting of the cathodic and anodic UPD peaks C_I and A_I is less in the presence of Cl$^-$ than in its absence, signifying that Cl$^-$ enhances the kinetics of Pb UPD deposition. Furthermore, the average position of the UPD peaks is closer to the bulk deposition potential in the presence of Cl$^-$, signifying that the binding energy of the UPD monolayer to the Cu substrate is less in this case [3]. The two cathodic UPD peaks C_{Ia} and C_{Ib} observed in CVs on polycrystalline Cu substrates may be associated with Cu sites having different geometries, as their separation in Fig. 2b is about 30 mV, which is close to the difference between the peak potentials for Pb UPD deposition on Cu(1 1 1) and Cu(1 0 0) in the presence of Cl$^-$ (-0.37 V and -0.40 V, respectively [3,6]).

Fig. 3a shows that the formation of the UPD Pb monolayer is clearly seen in the OI-RD signal. As a result of
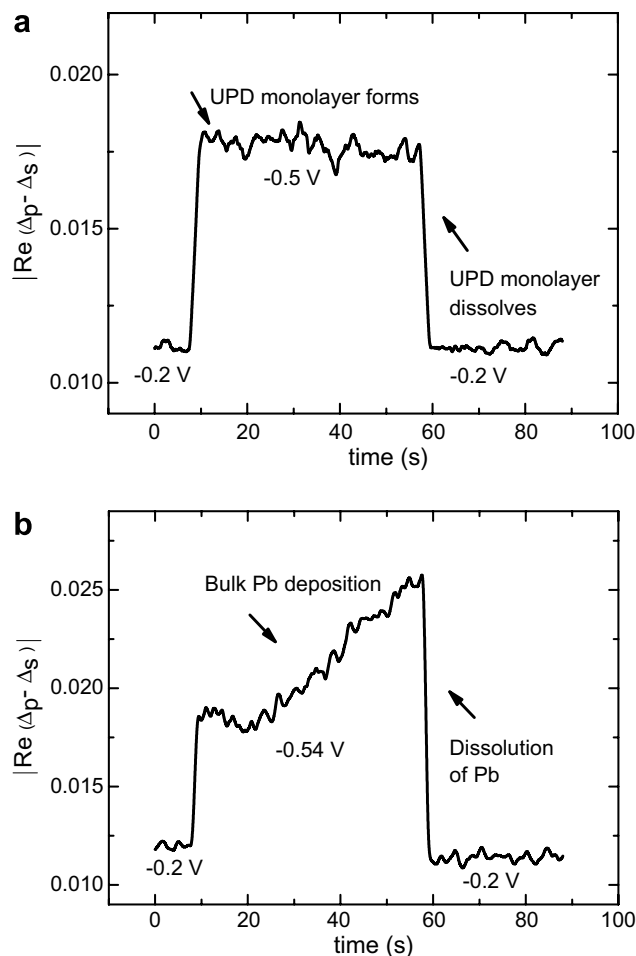
applying a potential $E = -0.5$ V (just positive of the bulk deposition potential) to the Cu substrate for $t = 50$ s in the absence of Cl$^-$, $|Re\{\Delta_p - \Delta_s\}|$ increases rapidly due to UPD Pb and then remains constant at the value corresponding to the UPD monolayer, indicating that there is no subsequent bulk Pb deposition. On returning the substrate potential to $E = -0.2$ V, the UPD monolayer dissolves and $|Re\{\Delta_p - \Delta_s\}|$ returns to its initial value. If a potential negative of the bulk deposition potential, $E = -0.54$ V is applied, Fig. 3b shows that OPD Pb (bulk deposition) causes $|Re\{\Delta_p - \Delta_s\}|$ to increase beyond the value corresponding to the UPD monolayer, after a few seconds delay (nucleation time). In situ AFM (Fig. 4) shows that numerous sub-micron Pb islands form at $E = -0.54$ V. The wide range of sizes observed suggests that nucleation is progressive. The sub-micron islands are seen to dissolve when the substrate potential is returned to $E = -0.2$ V.

In the presence of Cl$^-$, the OI-RD response during UPD has the same sign and order of magnitude as in the absence of Cl$^-$ (Fig. 5a). During OPD at $E = -0.54$ V, however,

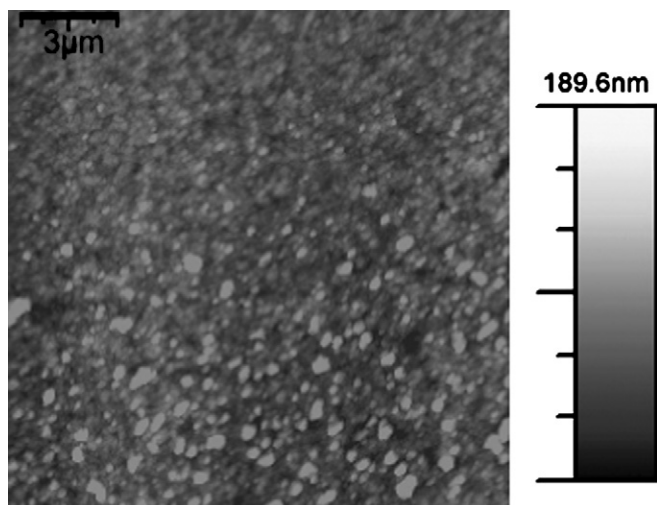Fig. 4. 15×15 μm in situ AFM image obtained in 100 mM HClO$_4$ + 1 mM Pb^{2+} electrolyte during growth at -0.54 V. The island size increases from the top of the figure (start of scan) to the bottom (end of scan) as growth proceeds.
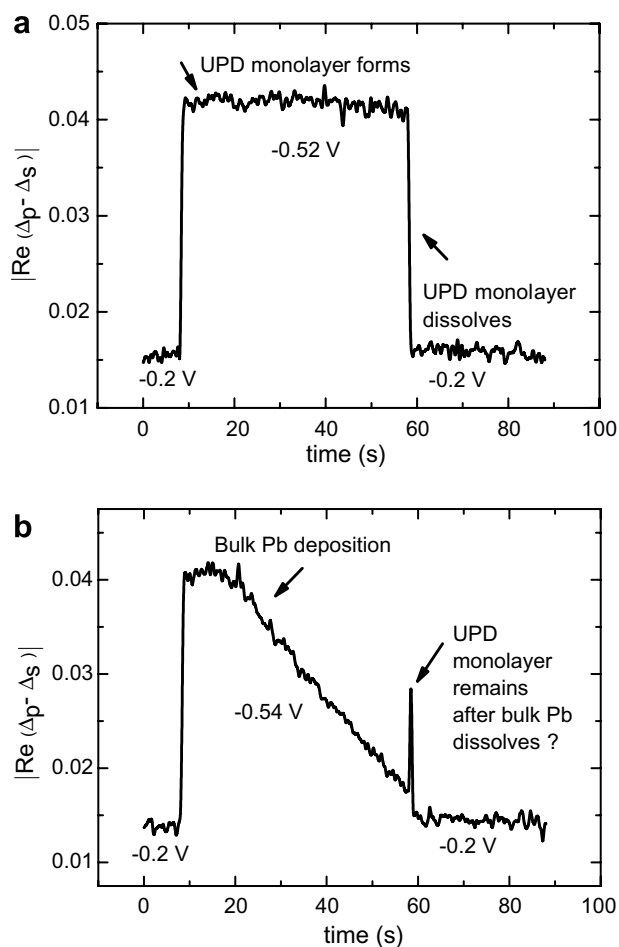

Fig. 5. OI-RD signal $|Re\{\Delta_p - \Delta_s\}|$ (not normalized) recorded when stepping the Cu substrate potential (a) from $E = -0.2$ V to $E = -0.52$ V for $t = 50$ s (UPD) and (b) from $E = -0.2$ V to $E = -0.54$ V for $t = 50$ s (OPD). The electrolyte was 100 mM HClO$_4$ + 1 mM Pb(ClO$_4$)$_2$ + 20 mM KCl.

there is a significant change. Fig. 5b shows that after completion of the UPD monolayer, $|Re\{\Delta_p - \Delta_s\}|$ starts to fall instead of continuing to rise. The opposing effects of the UPD and OPD layers on the OI-RD signal imply that the optical response of the material deposited at $E = -0.54$ V in the presence of Cl$^-$ is very different from that of the dense array of sub-micron islands deposited at this potential in the absence of Cl$^-$ (Fig. 4).

The reason behind the OI-RD response in the presence of Cl$^-$ is revealed by in situ AFM images (Fig. 6). There are tip artefacts in this image, but the differences in island size and density between this figure and Fig. 4 are obvious. In the presence of Cl$^-$, micron-sized Pb islands form with an average island-island separation of the order of 10 μm so that the surface is optically rough. From such a surface, the OI-RD signal is dominated by the disproportional scattering of s- and p-polarized light by the wavelength-sized and multi-wavelength-spaced Pb islands. This is because the efficiency for the s-polarized component to be scattered into the specular direction is markedly different from that for the p-polarized component. Our results so far suggest that nucleation in the presence of Cl$^-$ is instantaneous. Furthermore, when the substrate potential is cycled to deposit and re-dissolve OPD Pb, there is some evidence that islands form at the same locations in successive cycles, suggesting that they nucleate at defects.

Precisely why the presence of Cl$^-$ has such a drastic effect on the nucleation density of Pb islands during OPD remains to be established, but a possible explanation could be differences in the structure of the UPD layer in the presence and absence of Cl$^-$. Even though Cl$^-$ desorption has been reported in association with Pb UPD monolayer formation on Cu [3], our results make it seem likely that there is still Cl$^-$ adsorbed on the Pb prior to OPD deposition. XRD studies showed that the presence of Cl$^-$ had a non-negligible effect on the structure of the UPD monolayer, affecting both the degree of order and the Pb–Pb lattice
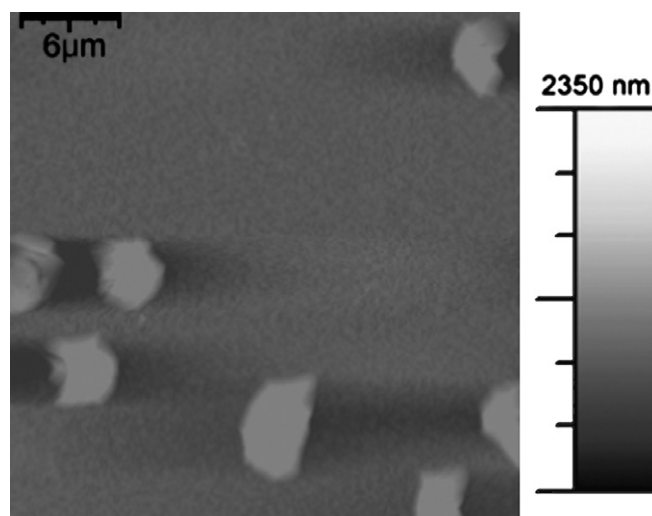

Fig. 6. 30×30 μm in situ AFM image obtained in 100 mM HClO$_4$ + 1 mM Pb^{2+} + 20 mM KCl electrolyte during growth at -0.54 V.

spacing as a function of potential [5]. Enhanced surface diffusion in the presence of Cl⁻ could also favour the formation of fewer larger islands. In any case, more work is required to establish any parallels with other systems.

Fig. 5b reveals a further interesting phenomenon. When the substrate potential is returned to $E = -0.2$ V, there is a spike in $|\text{Re}\{\varDelta_p - \varDelta_s\}|$ before the signal returns to its value prior to the start of Pb electrodeposition. This suggests that a compact Pb layer (for which the sign of $\text{Re}\{\varDelta_p - \varDelta_s\}$ is opposite to that of the sparse large islands) remains for a short time after the large islands dissolve. Our observation of this transitory effect is a nice example of how OI-RD and in situ AFM measurements complement each other, as it would be extremely difficult to interpret the OI-RD data without the AFM images, but our in situ AFM by itself has neither the spatial nor time resolution to reveal the persistence of the UPD monolayer after dissolution of the large islands.

At more negative deposition potentials, the shape of the $|\text{Re}\{\varDelta_p - \varDelta_s\}|$ transient is qualitatively similar in the presence and absence of Cl⁻, as seen from Fig. 7. Fig. 8b shows that the Pb islands that form in the presence of Cl⁻ at
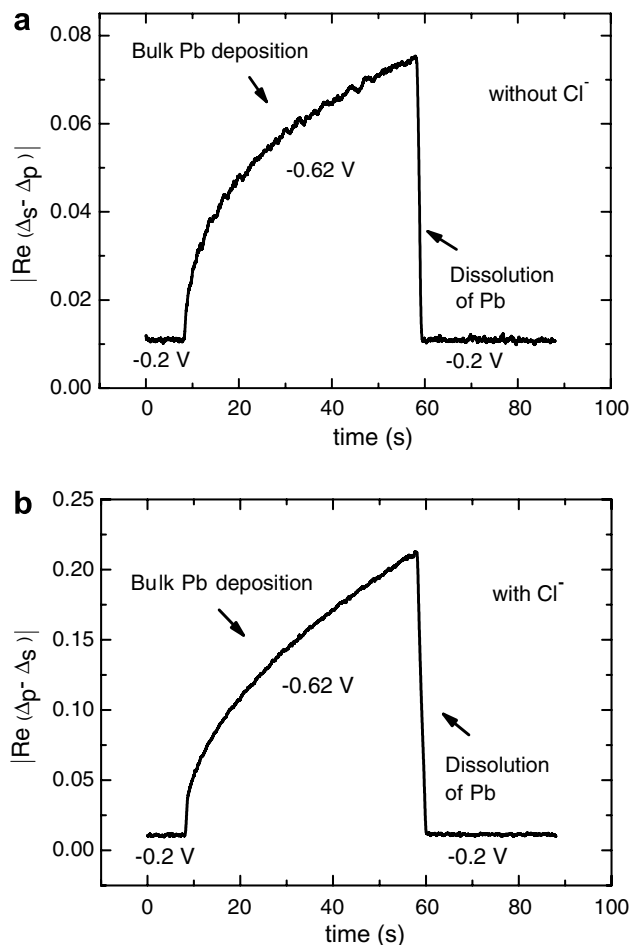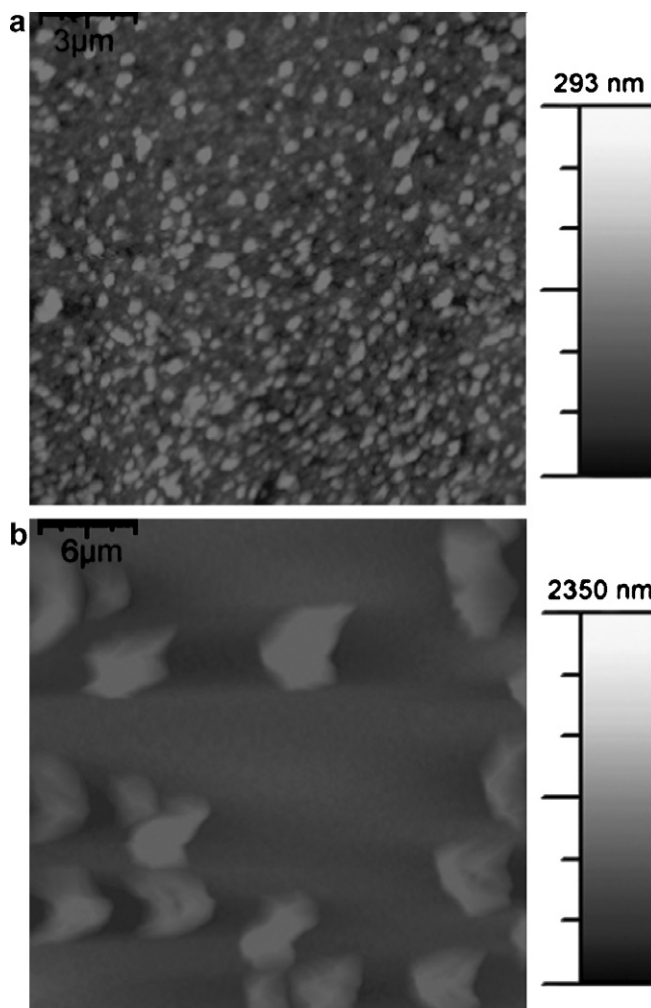

Fig. 8. (a) $15 \times 15\ \mu m$ in situ AFM image of islands formed by Pb deposition at $E = -0.62$ V in 100 mM HClO$_4$ + 1 mM Pb^{2+} electrolyte; (b) $30 \times 30\ \mu m$ in situ AFM image of islands formed by Pb deposition at $E = -0.62$ V in the same electrolyte + 20 mM KCl.

-0.62 V are of a similar size to those that form at $E = -0.54$ V and much larger than those that form in the absence of Cl⁻ at $E = -0.62$ V (Fig. 8a). However, the density of islands is greater than at $E = -0.54$ V. It appears to be the increased density of Pb islands that changes the effective dielectric constant to a value closer to that of a compact Pb film, which gives a monotonically increasing $|\text{Re}\{\varDelta_p - \varDelta_s\}|$ signal.

4. Conclusion

We have shown that the growth mode of bulk-phase Pb on polycrystalline Cu is heavily modified by the presence of Cl⁻ in the electrolyte. In the absence of Cl⁻, a high density of sub-micron sized islands forms and the OI-RD signal $|\text{Re}\{\varDelta_p - \varDelta_s\}|$ increases monotonically with increasing Pb coverage, as expected for a compact Pb film. In the presence of Cl⁻, large islands form, with lateral dimensions up to several μm. At low overpotentials, the island density is sufficiently low that $|\text{Re}\{\varDelta_p - \varDelta_s\}|$ decreases with

Fig. 7. OI-RD signal $|\text{Re}\{\varDelta_p - \varDelta_s\}|$ (not normalized) recorded when stepping the Cu substrate potential from $E = -0.2$ V to $E = -0.62$ V for $t = 50$ s (a) in 100 mM HClO$_4$ + 1 mM Pb(ClO$_4$)$_2$ and (b) in 100 mM HClO$_4$ + 1 mM Pb(ClO$_4$)$_2$ + 20 mM KCl.

increasing Pb coverage after formation of the UPD monolayer, while at higher overpotentials it increases monotonically, as in the absence of Cl^-. The origin of this dramatic change in growth mode is still under investigation, but could be associated with a change in the structure of the initial UPD monolayer. OI-RD data also suggest that when dissolving bulk Pb in the presence of Cl^-, a compact UPD monolayer persists for a short time after the disappearance of the large Pb islands. This phenomenon is only observed because of the high speed of OI-RD relative to our in situ AFM.

References

[1] B.J. Hinch, C. Koziol, J.P. Toennies, G. Zhang, Vacuum 42 (1991) 309.
[2] G. Meyer, M. Michailov, M. Henzler, Surf. Sci. 202 (1988) 125.
[3] G.M. Brisard, E. Zenati, H.A. Gasteiger, N.M. Marković, P.N. Ross Jr., Langmuir 11 (1995) 2221.
[4] G.M. Brisard, E. Zenati, H.A. Gasteiger, N.M. Marković, P.N. Ross Jr., Langmuir 13 (1997) 2390.
[5] Y.S. Chu, I.K. Robinson, A.A. Gewirth, Phys. Rev. B 55 (1997) 7945.
[6] T.P. Moffat, J. Phys. Chem. B 102 (1998) 10020.
[7] C. Nagl, O. Haller, E. Platzgummer, M. Schmid, P. Varga, Surf. Sci. 321 (1994) 237.
[8] C. Nagl, E. Platzgummer, O. Haller, M. Schmid, P. Varga, Surf. Sci. 331–333 (1995) 831.
[9] A. Wong, X.D. Zhu, Appl. Phys. A 63 (1996) 1.
[10] P. Thomas, E. Nabighian, M.C. Bartelt, C.Y. Fong, X.D. Zhu, Appl. Phys. A 79 (2004) 131.
[11] W. Schwarzacher, J. Gray, X.D. Zhu, Electrochem. Solid-State Lett. 6 (2003) C73.
[12] X.D. Zhu, Y.Y. Fei, H.B. Lu, G.Z. Yang, Appl. Phys. Lett. 87 (2005) 051903.
[13] J.D.E. McIntyre, D.E. Aspnes, Surf. Sci. 24 (1971) 417.
[14] X.D. Zhu, Phys. Rev. B 69 (2004) 115407.